IOP Conf. Series: Materials Science and Engineering **448** (2018) 012059 doi:10.1088/1757-899X/448/1/012059

Investigation of constitutive equation parameters on dual phase steel sheets

G Béres[1] and M Tisza[2]

[1]John von Neumann University, Faculty of GAMF Engineering and Computer Science, Department of Materials Technology, 10. Izsáki road Kecskemét 6000 Hungary.
[2]University of Miskolc, Faculty of Mechanical Engineering and Informatics, Institute of Materials Sciences & Technology, Miskolc-Egyetemváros 3515 Hungary.

beres.gabor@gamf.uni-neumann.hu

Abstract. This study is about using of the least squares' method for parameter defining and model accuracy investigation of mechanical-based work-hardening laws of automotive dual phase steels. The experimental true stress true strain curves were determined by standard, quasi-static tensile tests at room temperature. As most of the commercial finite element codes are using mechanical-based constitutive equations for describing the stress-strain relationship of the materials, the coefficients of these equations are one of the most important input parameters of the simulations. The results show that most of the models are able for data estimation, but the physical meaning of each model parameters is not taking into account by this mathematical technique. The highest of the stress values are observed at Ludwik's solution, while the lowest are given by the Voce model at each steel grades. Although the differences are negligible in the strain range of uniform elongation, but significant discrepancies are displayed at higher strains, which typically occur during sheet forming processes in the press shop. The model parameters' developing in the function of the martensite volume fraction was also considered.

1. Introduction

Finite element (FE) analysis is a useful technique for evaluation of metal forming processes. The success of these simulations is significantly depends on the accuracy of the input parameters. One of the most important input parameter of FE simulations is the flow curve of the material. Current FE codes contain more types of integrated equations in which the accuracy of each parameters are generally depending on the approximation method of the measured stress-strain values. The best-known mechanical approximations models are originated from such famous scientists like Nádai [1], Zener and Hollomon [2], Ludwik, Swift [3], Voce [4], Johnson and Cook [5], as well as Hockett and Sherby [6]. These researches elaborated their equations in different mathematical concepts, due to the complexity of the deformation process of metals. Nevertheless, this complexity is the reason why the understanding of exact processes which happen in the microstructure during plastic deformation is still actual topic at metallic materials.

The applied automotive dual phase (DP) steels are widely used in the automotive industry due to their beneficial attributions, not only in the field of forming but in the field of joining technologies like welding [7] or soldering [8,9] also. These steels contain soft ferrite and hard martensite in the

microstructure, thus the mechanical properties are mainly depending on the amount, the morphology and the distribution of each phases [10]. Consequently, the microstructure-based modelling of these steels is also a popular field, so new hardening model strategies are continuously spreading with the development of computer performance and microscopic techniques. This modelling means the mechanical simulation of each phases of the microstructure, taking into account the microscopic properties like grain size, dislocation density, length of the burgers vector, etc. The method is called as representative volume element (RVE) technique [11,12,13].

Although, these materials are particularly appropriate for RVE simulations (as the mechanical properties can be defined well by the amount, the morphology and the distribution of each phases), we primarily focused on the accuracy of the classic, mechanical-based approximation methods.

2. Materials and experiments

Three types of conventional DP steels as DP600, DP800 and DP1000 with the chemical composition and phase proportions (i.e. ferrite and martensite volume fractions) shown in table 1 were applied in this study. The chemical compositions were defined by optical spectrometry. For the microstructure analysing and the calculation of the phase dispersions, small pieces were grinded and polished by using standard metallographic sample preparation techniques and then etched in 2% nital. The calculation of the area ratios in percent of each phases were performed by the usage of Zeiss Imager M2m program wizard software, in at least five different cross sections. Figure 1 shows some specific microscopic pictures of each sample. It is worthy to note that DP800 has a bit higher average carbon content than DP1000. It is contrary to the general experiences, that higher martensite volume fraction (MVF) belongs to higher carbon content.

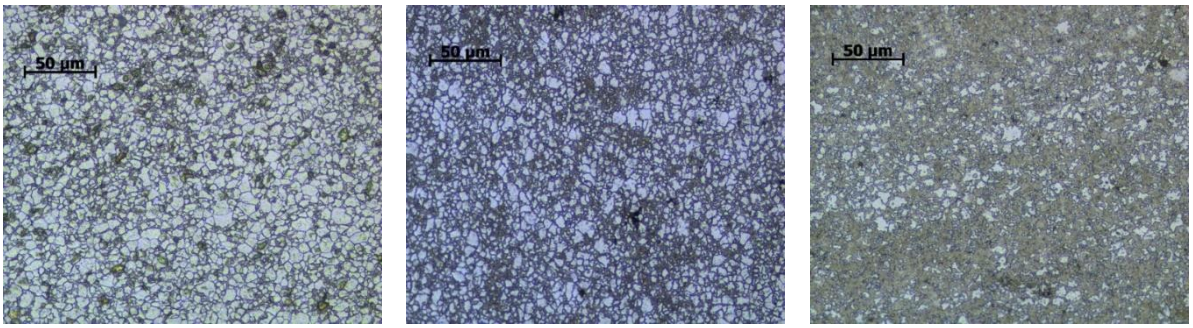

(a) (b) (c)

Figure 1. Microstructure of (a) DP600, (b) DP800 and (c) DP1000 materials, etched in 2% nital.

Table 1. Chemical composition of the applied DP steels.

	Fe (wt%)	C (wt%)	Si (wt%)	Mn (wt%)	P (wt%)	S (wt%)	Ferrite vol.%	Martensite vol.%
DP600	98.6	0.085	0.171	0.87	0.013	0.005	0.734	0.266
DP800	97.9	0.161	0.187	1.52	0.012	0.003	0.579	0.421
DP1000	97.8	0.148	0.181	1.50	0.012	0.004	0.350	0.650

The engineering stress engineering strain (e) curves were determined by tensile tests according to MSZ EN ISO 6892-1:2010 European standard, with 30 mm/min frame rate at room temperature. The tensile specimens with gauge length of 80 mm and 1mm thickness were manufactured based on the mentioned prescription in three directions: parallel, perpendicular and 45° to the rolling direction. The measurements in all different specimen conditions were repeated five times. For the strain measuring we used contact proof AVE video extensometer. The calculation method from engineering data (across tensile force – F_i and initial cross section – A_0) to true data is well-known and given by equation (1) and (2). As these materials show near isotropic behaviour and constant thickness-transverse strain

development during outer loading (figure 2 (d)), only the results of specimens parallel to the rolling direction can be seen in details, in the coordinate system of true and equivalent quantities (figure 2 (a) – (c)). The isotropic behaviour is also demonstrated by the $\bar{r}$ value. The main mechanical properties are summarized in table 2.

$$\sigma_{eq} = \frac{F_i}{A_0}(1+e) \quad (1)$$

$$\varepsilon_{eq} = \ln(1+e) \quad (2)$$

Table 2. The main mechanical properties of the applied DP steels.

	UTS N/mm²	YS N/mm²	A_{80} (%)	Ag (%)	ε_{total}	ε_{crit}	$\bar{r}$
DP600	656	445	20.6	13.6	0.187	0.128	0.92
DP800	879	571	16.0	10.8	0.148	0.102	0.75
DP1000	1099	767	10.6	7.0	0.101	0.067	0.76

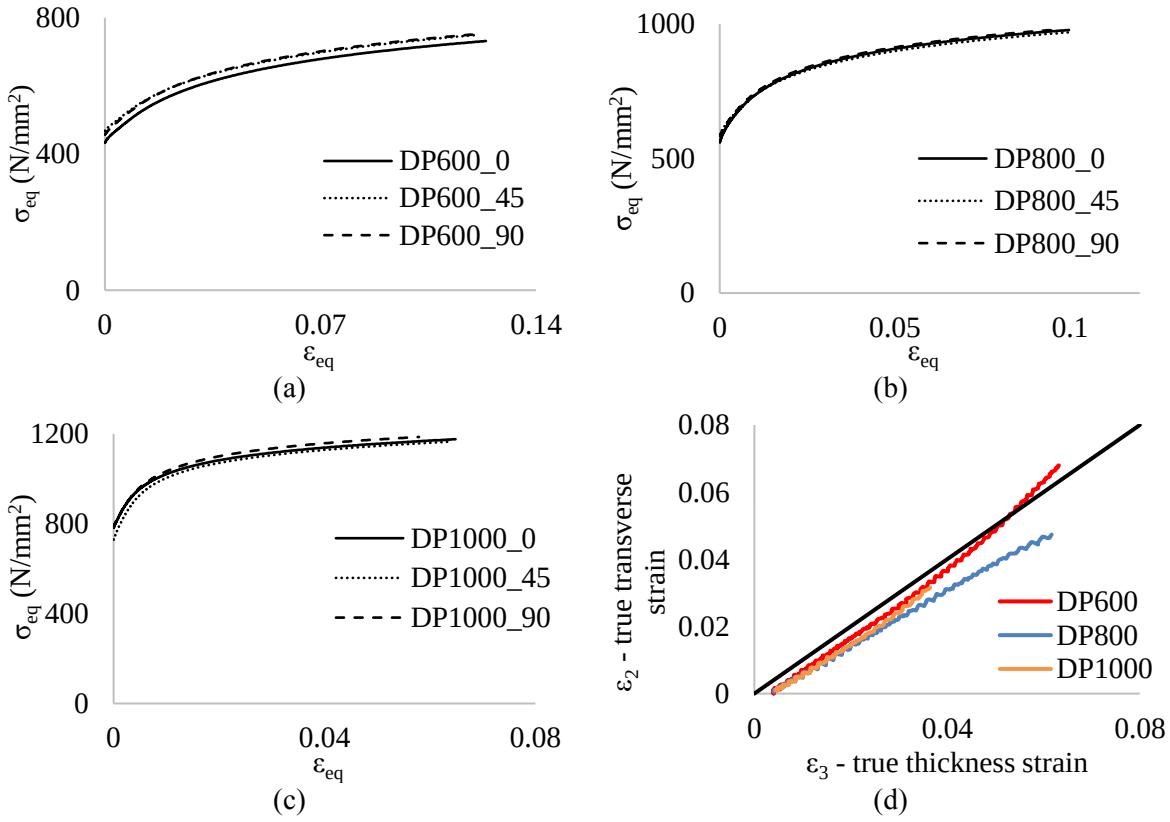

Figure 2. Flow curves of DP600 (a), DP800 (b) and DP1000 (c) materials and the true thickness – true transverse strains developing during the tensile test (d).

In table 2, Ag belongs to engineering uniform strain, while ε_{total} is the total true and ε_{crit} is the uniform true strains. In the same place, $\bar{r}$ means the Lankford coefficient.

3. Parameter fitting by the least squares' method

The parameter fitting of each flow curve model equations were performed by the least squares' method. The least squares' method is a mathematical method to calculate the differences of the estimated ($\check{y}_i$)

and the measured values (y_i) of a given function. The object is the minimizing of the sum of the squared errors (χ^2), which is the square of the differences of the values mentioned above (3).

$$\chi^2 = \sum(\check{y}_i - y_i)^2 \tag{3}$$

With the appropriate changing of the parameters between the iteration steps in the mathematic solver program, the most accurate estimation can be available. The estimation accuracy is generally defined by the quadratic regression (4), which already contains the value of the sum of the squared totals (SST in equation (5)) next to the χ^2. It is worthy to mention, that one of the main disadvantage of this method is that the results are slightly depending on the user defined initial value of the predicted function. Fortunately, now it does not mean serious problem, as the start points of the estimated curves are known, as the initial yield strength of the materials.

$$R^2 = \frac{SST - \chi^2}{SST} \tag{4}$$

$$SST = \sum(y_i - \bar{y})^2 \tag{5}$$

The fitted stress-strain curves according to five different theories as well as the experimental data with different colors can be seen in figure 3 respectively, for DP600, DP800 and DP1000 materials.

It is observed that all the theories can approach the experimental results with sufficient accuracy in the strain range of uniaxial tension (table 3). Nevertheless, the models can show definite discrepancies at higher strains. It can be made visible with the extension of the strain axis up to the possible strain values at equi-biaxial tension. So as the figures below point it out, the solution of Ludwik calculates the highest stresses, while the Voce and Hockett-Sherby models calculate the lowest stresses for each strain values, for all investigated steels.

Table 3. The estimation accuracy as the quadratic regression values for the different models.

	R^2				
	Nádai	**Ludwik**	**Johnson-Cook**	**Voce**	**Hockett-Sherby**
DP600	0.8949	0.9860	0.9930	0.9936	0.9995
DP800	0.9332	0.9758	0.9894	0.9881	0.9991
DP1000	0.8790	0.9495	0.9790	0.9857	0.9969

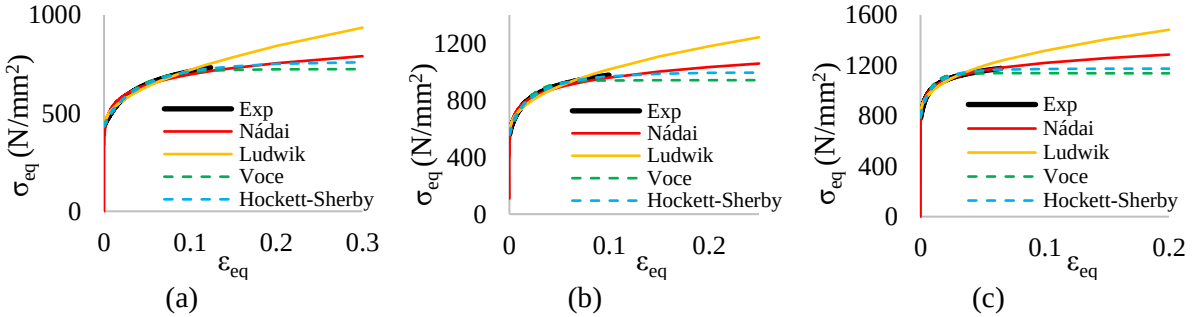

Figure 3. Experimental ("Exp") data and the fitted flow curves' offset for DP600 (a), DP800 (b) and DP1000 (c) steels.

4. Discussion

One classic constitutive model (6) is originated from Nádai [1], which was expanded later with a constant value (A in equation (7)) refers to the yield strength by Ludwik [3]. Similar expanding with an added constant but not refers to the yield strength is originated from Swift [3] (not published here). Former equation is often attributed to the names of Zener and Hollomon also. They reported more studies [2,14,15] about the stress-strain relationship of steel materials and about the effect of the strain

rate and temperature, still in the negative degrees also. The genesis of these papers are nearly the same as the paper of Nádai.

$$\sigma_{eq} = K\varepsilon_{eq}^{n} \tag{6}$$

$$\sigma_{eq} = A + K\varepsilon_{eq}^{n} \tag{7}$$

The physical meaning of the n exponent in the Nádai expression can be described as the value of the uniform equivalent strain belonging to the onset of local necking (ε_{crit}) and as the steepness of the linear relationship between the stresses and strains in the logarithmic coordinate system (8). Therefore, it should remain a constant value during the uniform deformation process. Nevertheless, in the case of DP steels, due to the non-proportional deformation of the ferrite and martensite phases [16], it cannot be realized in the practice. Figure 4 visualizes the changing of Nádai and Ludwik exponents respectively in the function of the MVF fraction. The figures indicated the logarithmic axial strain at the onset of neck formation also (ε_{crit}).

$$\ln(\sigma_{eq}) = \ln K + n \cdot \ln(\varepsilon_{eq}) \tag{8}$$

$$\ln(\sigma_{eq} - A) = \ln K + n \cdot \ln(\varepsilon_{eq}) \tag{9}$$

In the Ludwik approximation, this exponent receives a quiet new meaning, and mostly differs from the limit uniform axial strain. Besides, the n exponent also should hold the linear relationship not between the logarithm of stresses and strains, but between the differentiation of the logarithm of tensile stress and of A parameter, and the logarithmic tensile strain (9). The higher discrepancies in figure 5 appear at the lower strains, as only the ferrite phases deform in the early progress. Later, the strain dispersion increasingly homogenised, as the low carbon content martensite also start to deform slightly.

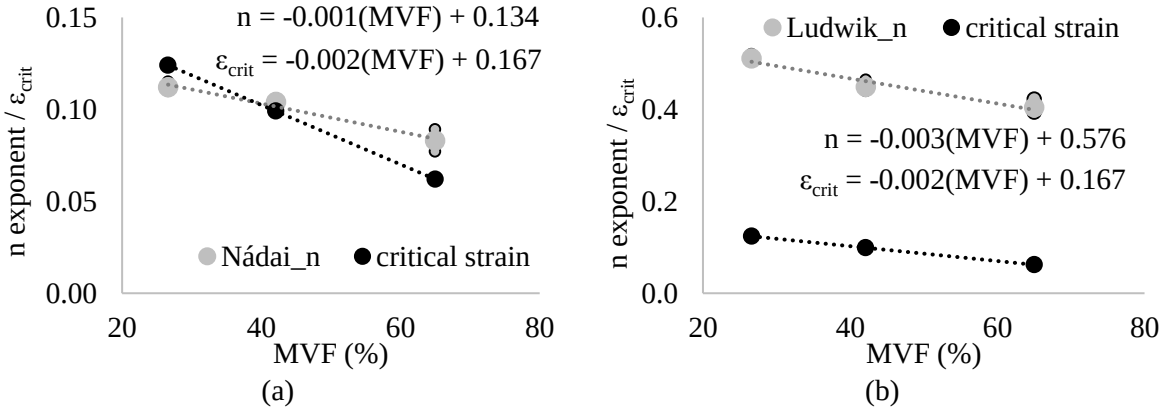

Figure 4. Changing of the n exponent according to the expressions of Nádai (a) and Ludwik (b) moreover the critical axial true strains depending on the MVF.

The shown examples refer to specimens manufactured in the rolling direction again. The calculated straights are presented as continuous lines - black line for Nádai and grey line for Ludwik approximation - while the measured values are symbolized by colourful dot series - red dots for Nádai and green dots for Ludwik approximation. It can be seen, that with the increasing of the MVF, the inhomogeneous deformation, thus the deviation of the measurements from the calculated straights are increasing.

Even let us here to mention, that the values of the n exponent show similar decreasing in both equations, with the growing of the MVF of the material. Regarding the mean values, with the changing of the MVF with 0.58% and 0.54% from DP600 to DP800 and from DP800 to DP1000 respectively, the changing of the exponents produces ~10% and ~20% decreasing in case of the Nádai, as well as ~12% and ~10% decreasing in case of the Luwik-type equations.

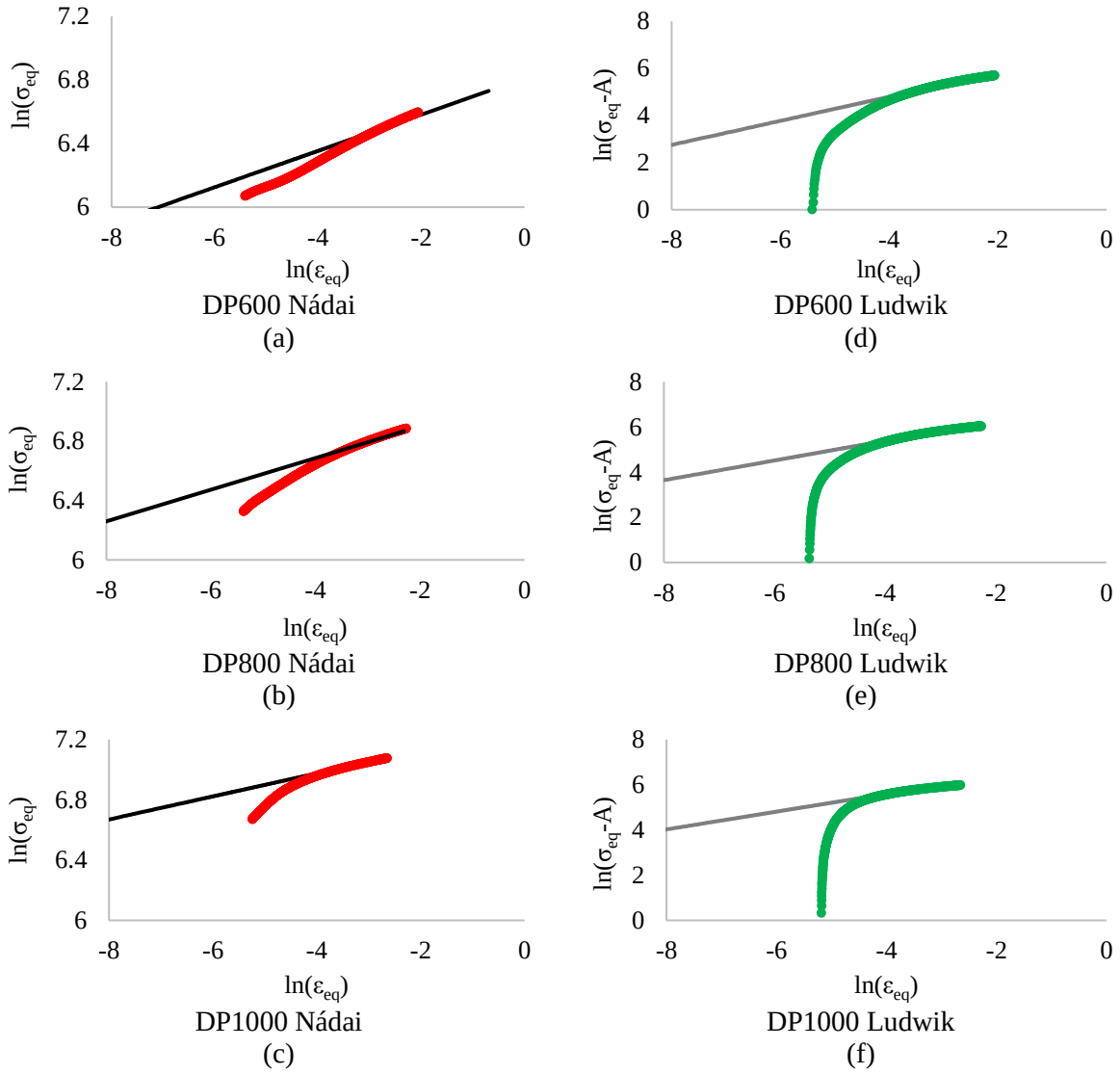

Figure 5. The calculated (black and grey straights) and the measured (colorful dots) stress-strain pairs in the log-log coordinate systems.

Next to conventional power laws, we investigated the compliance of strain-rate sensitive models also. The Ludwik solution gives the basis of two rate-dependent models, one from Jonson-Cook [5] and the other from Cowper-Symonds [17]. Former one attaches the strain rate to the plastic deformation by a logarithmic relationship (10). They performed high number of high strain rate dynamic tests subjected to large strains in twelve different grades of materials, during the experimental validation. Their constitutive model contains the effect of the thermal softening also with exponent of 'm'. Since the effect of the temperature is ignored in this study, only isothermal condition, in this way only the effect of the strain rate multiplier (C) in the function of the MVF is considered.

$$\sigma_{eq} = \left[A + K\varepsilon_{eq}^{n}\right]\left[1 + C \cdot \ln(\dot{\varepsilon}_{eq})\right] \tag{10}$$

$$\sigma_{eq} = \left[A + K\varepsilon_{eq}^{n}\right]\left[1 + \left(\frac{\dot{\varepsilon}_{eq}}{D}\right)^{1/p}\right] \tag{11}$$

Although, Johnson and Cook used much higher strain rates ($\dot{\varepsilon}_{eq}$) than we did, the calculated values of the multiplier (C) fell enough far from the experimental results in different strain rates. In their paper,

this multiplier connected the stresses to the logarithm of the strain rates, up to 1000 1/s. We used 0.4 mm/min, 4 mm/min, 40 mm/min and 400 mm/min cross head speeds to make some observation on the behaviour of this parameter. Considering the 80 mm gauge length of the specimens, it means that all of the applied strain rates were well below the unity 1/s, which logarithm is below than zero. It could be the reason, why the measured values of DP600 steels were two orders of magnitude higher, than the values were accepted by the least squares' method (figure 6).

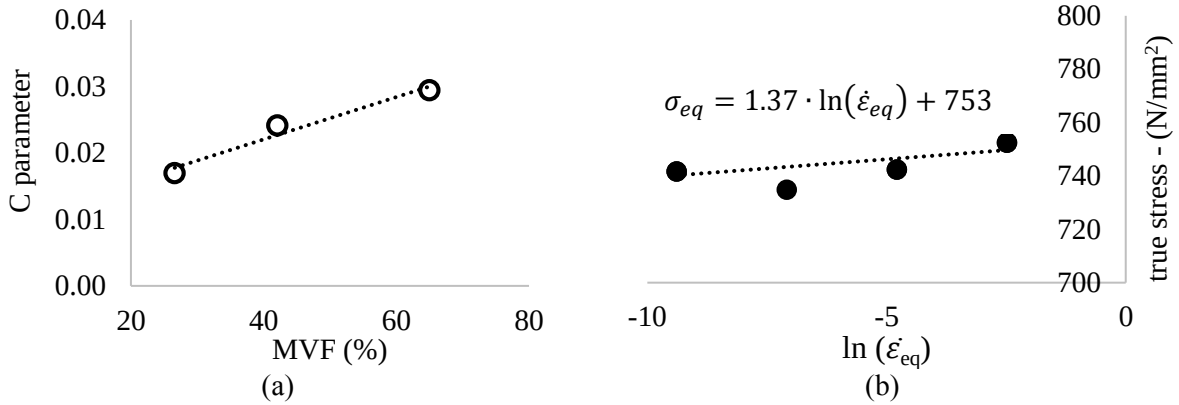

Figure 6. The calculated C parameters in the Johnson-Cook expression in the function of the MVF (a), and the experimental result of C with different cross head speeds (b) for DP600.

Cowper and Symonds calculated the effect of the strain rate through the pth root form equation (see equation (11)). This form of strain rate dependency does not change significantly the approximated results, since the D parameter came to very close to unity and the p exponent came to around 0.25. For as much the term in the second bracket is actually so close to unity, which means that no noticeable different was born compared to Ludwik's expression.

Voce [4] examined stress-strain curves for Cu and its alloys to true strain not beyond -1.0 (compression). Although, he firstly introduced an exponential relationship between the stress-strain values maybe, but such limited strain data made his correlation difficult to establish reasonable parameters for large strains. Voce's model is described by equation (12).

$$\sigma_{eq} = A + q[1 - \exp(-b\varepsilon_{eq})] \tag{12}$$

$$\sigma_{eq} = \sigma_s - \exp\left(-N\varepsilon_{eq}\right)^p (\sigma_s - A) \tag{13}$$

Some decades later, Hockett and Sherby [6] proposed that cell formation dominates the plastic flow process, and got similar equation this way than Voce. They introduced the concept of steady-state flow stress for large strains (σ_s in (13)). They assumed that a steady-state flow stress (and consequently a steady-state microstructure) can be approached asymptotically, so that is why the true stress is approximated by a pth exponential form. Note that if the value of p in equation (13) is taken as unity, the Voce and Hockett-Sherby models are identical.

For these DP steels, p parameter is nor got as unity neither as 0.58, as it was supposed by Hockett and Sherby for α-Fe. The similarity of the varying of the strain multiplying factors (b and N) for Voce as well as Hockett-Sherby relationships is well visible in figure 7 (a). Both can be fitted quite well by exponential approximation with the growth of MVF. The same figure depicts the p exponent and the q multiplier (b) as well as the steady-state flow stress value (d) likewise in the function of the MVF. σ_s is able to well fitted by a power law, just like the K parameter of the former equations (c). In turn, there is a local minimum on the curve of the varying of the p exponent, and there is a local maximum on q, but no reasonable relationships are possible to determine in the function of MVF.

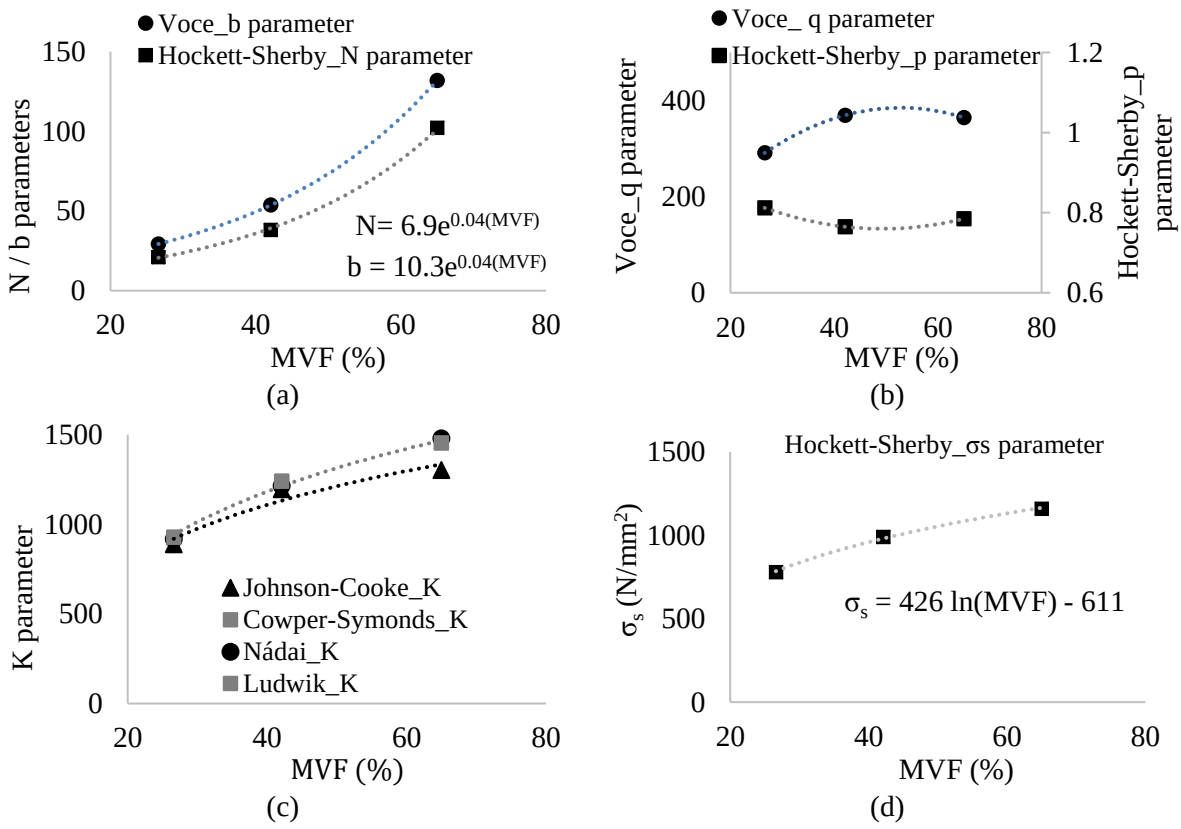

Figure 7. Predicted model parameters in Voce's and Hockett and Sherby's equations (a, b, d) and the K parameter (c) in the function of MVF.

5. Summary

This paper presents the experimentally determined and mathematically fitted flow curves of three types of dual phase steels. It can be observed that all the published constitutive laws are able to properly describe the stress-strain relationship using of least squares parameter fitting, besides, there are no significant discrepancies in the strain-range of uniaxial tension. Nevertheless, considerable disparities may occur between the models at larger strains, in which the Voce model estimate the lowest, and the Ludwik model estimates the higher stresses for the same strain data, in case of all steels. The differences will be well visible with the strain data offsetting up to such an equivalent strain value, which can typically occurs during biaxial tension.

Furthermore, the parameter sensitivity for the martensite volume fraction (MVF) was also displayed. It can be stated that all of the strain multipliers like K, b, N as well as the strain rate multiplier (C) and the one stress featured parameter (σ_s) of the models were always increasing with the increasing of the MVF. Only for the q and p parameters in the Voce and Hockett-Sherby models could not be found any functional relationship with the MVF.

Acknowledgement

This research is supported by EFOP-3.6.1-16-2016-00006 "The development and enhancement of the research potential at John von Neumann University" project. The Project is supported by the Hungarian Government and co-financed by the European Social Fund.

References

[1] Nádai A L 1937 *J. Appl. Phys.* **8** pp 205–213.

[2] Zener C, Hollomon J H 1944 *J. Appl. Phys.* **15** pp 22
[3] Kim S, Lee J, Barlat F, Lee M-G 2013 *Journal of Materials Processing Technology* **213** pp 1929–1942
[4] Voce E *J. Inst. Metals* **74** pp 537
[5] Johnson G R, Cook W H 1985 *Engineering Fracture Mechanics* **21** pp 31-48
[6] Hockett J E, Sherby O D 1975 *J. Mech. Phys. Solids* **23** pp 87-98
[7] Berczeli M, Buza G 2017 *Materials Science Forum* **885** pp 178-183
[8] Gergely G, Koncz-Horvath D, Weltsch Z, Gacsi Z 2017 *Archives of Metallurgy and Materials* **62**:(2) pp 1033-1038
[9] Berczeli M, Weltsch Z 2018 *Periodica Polytechnica-Transportation Engineering* **46**:(2) pp 63-68
[10] Uthaisangsuk V, Prahl U, Bleck W 2011 *Engineering Fracture Mechanics* **78** pp 469–486
[11] Perzynski K, Madej L 2017 *Arch Computat Methods Eng* **24** pp 869–890
[12] Perzynski K, Wrożyna A, Kuziak R, Legwand A, Madej L 2017 *Finite Elements in Analysis and Design* **124** pp 7–21
[13] Madej L 2017 *Archives of Civil and Mechanical Engineering* **17** pp 839-854
[14] Zener C, Hollomon J H High speed testing of mild steel *Am. Soc. Metals, in print*
[15] Zener C, Hollomon J H Plastic flow and rupture in metals *Am. Soc. Metals, in print*
[16] Kalashami G, Kermanpur A, Ghassemali E, Najafizadeh A, Mazaheri Y 2016 *Materials Science & Engineering A* **678** pp 215–226.
[17] ANSYS Inc. Release Notes 18.0, Structures with Material Nonlinearities, Rate-independent Plasticity